JOURNAL OF MATERIALS SCIENCE 14 (1979) 2205–2214

Indirect detection of grain-boundary segregation of carbon in iron-chromium alloys (Cr 10%) by electrochemical study

DANIÈLE BOUCHET, LOUISETTE PRIESTER
Laboratoire de Métallurgie Physique, associé au CNRS no. 177, Université de Paris-Sud, Centre d'Orsay, 91405 Orsay Cedex, France

The electrochemical behaviour of ferritic iron–chromium alloys is strongly dependent on the quantity (even in trace amounts), the localization in the microstructure and the chemical state of impurities. By comparing the direct and reverse anodic curves of alloys with different microstructures, it is possible to distinguish the respective influences of carbon segregation and carbide precipitation on the formation and the destruction of passive film. Reciprocally, in some cases, the anodic curves can be used to detect micro segregations at grain boundaries whereas no microanalysis can yet achieve this. This possibility is very interesting because many properties of alloys are largely determined by the presence of grain-boundary segregation without precipitation.

1. Introduction

In his recent assessment of investigative techniques of segregation Hondros pointed out the importance of electrochemical properties of interfaces compared with those of the bulk [1]. The aim of this paper is to show an example of the possible electrochemical approach of grain-boundary segregation and to assess the advantages of proceeding further in this direction. It is based on a better understanding of the relation between the microstructure and the anodic polarization curves of alloys.

2. Experimental procedures

2.1. Materials

The materials studied were iron–chromium alloys with chromium contents less than 12% containing traces of impurities, especially carbon and nitrogen. They were subjected to different heat-treatments, in order to obtain variations in the distribution of interstitials:

(1) the samples were annealed at 1200° C and then quenched; under these circumstances, carbon and nitrogen are completely in solid solution in the ferrite;

(2) some of the previous alloys were strongly cold-worked, then recrystallized at 780° C for 3 days. This temperature was chosen because it is situated in the high part of the α region of the equilibrium diagram (Fig. 1) and it is likely to obtain a well equilibrated ferrite structure. In this ferrite, nitrogen is completely insoluble whereas the solid solubility of C is 15 ppm [2];

(3) the other alloys were annealed at 1000° C and slowly cooled to room temperature. The

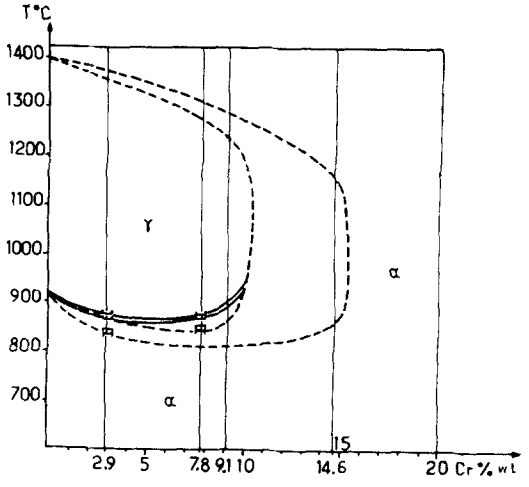

Figure 1 Equilibrium diagram of iron–chromium alloys.

0022–2461/79/092205–10 $03.00/0 © *1979 Chapman and Hall Ltd.*

ferrite obtained by the transformation $\gamma \rightarrow \alpha$ contains many precipitates surrounded by depleted chromium areas.

For each chromium content and for each heat-treatment, two degrees of purity of the alloys were compared:

alloys E: $\%C \leqslant 20$ ppm
$\%N < 4$ ppm

alloys P: $\%C \simeq 50$ ppm
$\%N \simeq 50$ ppm.

2.2. Potentiokinetic curves

The anodic curves of the alloys were determined in 7 N sulphuric acid with a polarization rate of $2\,V\,h^{-1}$. Before considering the electrochemical behaviour of the alloys it is necessary to know that of pure iron and pure chromium, which are quite different.

For pure iron, three parts can be distinguished on the anodic curve (Fig. 2a):

(1) active dissolution up to E_C; the Fe^{2+} ions go into solution;

(2) pre-passivation between E_C and E_F; a not fully protective layer is formed on the surface. Its nature depends on the electrolyte and on the pH; it could be $FeSO_4$ and/or $Fe(OH)_2$ [3, 4];

(3) passivation then occurs: a really protective amorphous layer is formed, seen by most electrochemists as the oxide Fe_2O_3 [5].

The behaviour of chromium is more simple. The passive Cr_2O_3 film is formed directly, without an intermediate state (Fig. 2b).

It is well known that the passivation of the alloys is improved as the chromium content increases; *inter alia,* the pre-passivation stage shortens. Initially, the alloys can be classified into three groups:

$0\% \leqslant Cr \leqslant 7.2\%$: the anodic behaviour is mostly of the iron type. Thus the pre-passivation stage presents current oscillations characteristic of $FeSO_4$ (Fig. 2a);

$7.2 < \%\,Cr \leqslant 10\%$: the anodic curve presents two peaks, E1 (activity peak) and E2 (passivation peak) (Fig. 3); the intensity of E_2 decreases as the chromium content increases;

$Cr > 10\%$: the passivation is almost of the chromium type.

2.3. Complementary techniques

Simultaneous to the plotting of the anodic curves, the following experiments were performed.

(1) Observation of the microstructure by electron microscopy at 100 and 1000 kV. The latter voltage was required because thicker foils can more reliably be compared with the samples used in the electrochemical study.

(2) Spectrographic analysis of carbon and nitrogen.

(3) Microanalysis of chromium by STEM. The spatial resolution can be evaluated at 500 Å and the level of detectability is about 0.5% Cr.

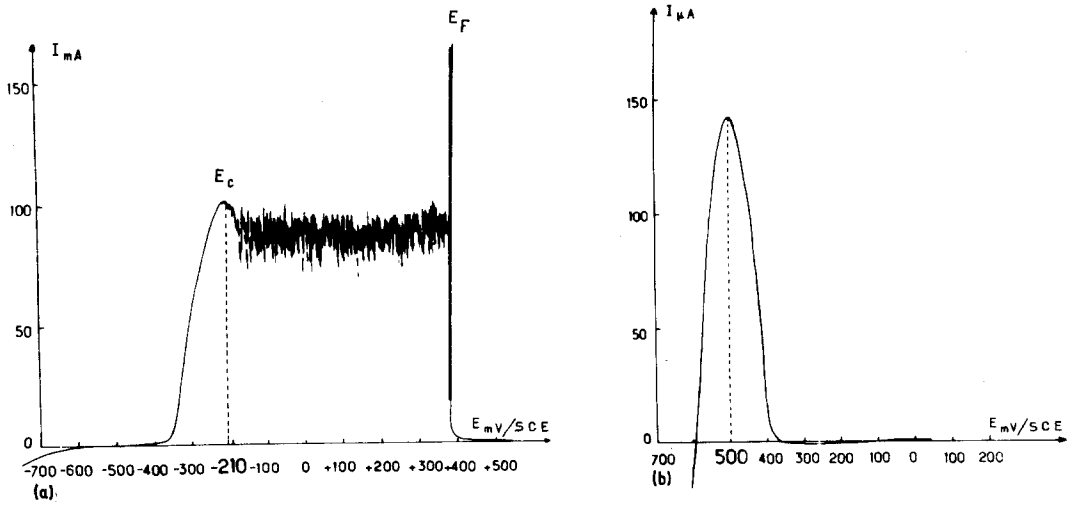

Figure 2 Experimental anodic polarization curves: (a) of iron; (b) of chromium. Electrolyte 7 N H_2SO_4, $V = 2\,V\,h^{-1}$.

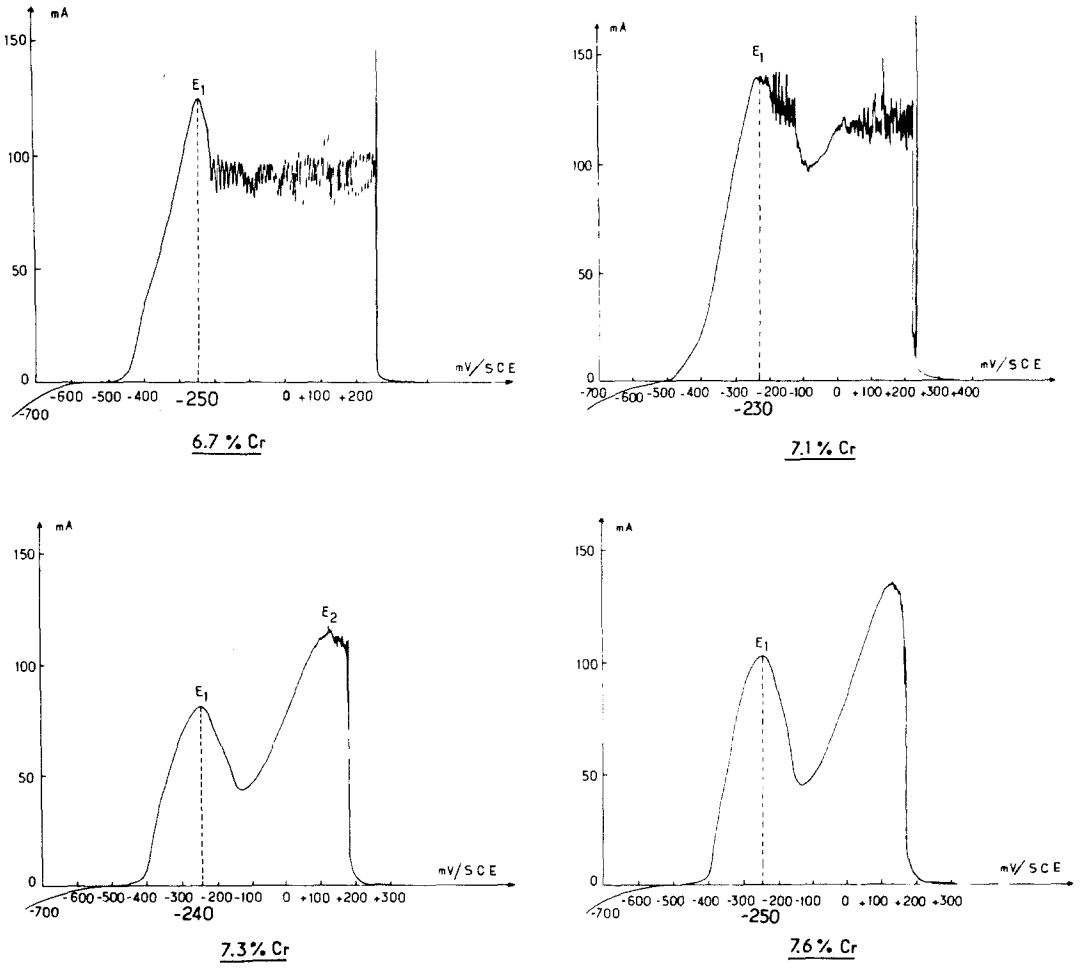

Figure 3 Transition of iron type anodic behaviour to that of the chromium type for alloys containing from 6.7% to 7.6% Cr.

(4) Micromicrodiffraction by STEM to attempt to detect microprecipitates.

(5) Observation by SEM or by TEM of replicas of the etched surface of samples using a suitable potential of attack.

(6) High-resolution autoradiography of ^{14}C to obtain information on the localization of carbon [6]. Before heat-treatment, about 20 ppm ^{14}C were introduced into the sample by decomposition of radioactive $BaCO_3$. The surface was then coated with a monogranular layer of a specific photographic emulsion sensitive to the β particles emitted by the decay of ^{14}C. These experiments were performed on thick samples with replicas, or on thin foils. In the first case, the replica and the photographic film were removed together from the surface and observed in the electron microscope. In the second case, the thin foils were first coated with a collodion layer to avoid the interaction between the photographic emulsion and the metal. After developing, the microstructure displaying carbon segregation could be observed much better than previously.

The presence of carbon is established by the observation of silver grains over the thin foil as a result of the interaction of the β particles with the photographic emulsion. The resolution, ρ, depends on a geometrical parameter and on a photographical one. The latter is almost the same for replica and thin foil but the geometrical resolution is strongly enhanced in thin foil because the range of β particles within the metal is shortened: $\rho = 1300$ Å.

Autoradiography on thin foil has better resolution, but a statistical approach is necessary and thus requires observation of replicas or, more recently, autoradiography of the surface of thick samples by SEM.

3. Results and discussion

All the results are explained by considering three basic notions: (1) the solid solubility of carbon and nitrogen in alloys at the annealing temperature; (2) the thermodynamic activity of chromium in the ternary alloy Fe–Cr–C which is expected to be strongly dependent on carbon content [7]; (3) the enrichment factor

$$\beta = \frac{\text{C content in the boundary}}{\text{C content in the grain}}.$$

The plan of the results is based on the metallurgical parameters which are classified into three groups depending on their influence on the anodic behaviour:

(1) difference in quantity of carbon (and/or nitrogen) in solid solution in homogeneous alloys;

(2) grain-boundary segregation of carbon in alloys which are still homogeneous in chromium;

(3) precipitation of carbides (and nitrides) surrounded by depleted chromium areas.

3.1. Electrochemical behaviour of homogeneous alloys

Whatever the purity E or P of the alloys, carbon and nitrogen are completely in solid solution after annealing the samples at 1200° C and quenching. In this case, for each chromium content other than 0% $E_{1E} < E_{1P}$ by about 40 mV. Because the activity peak of pure iron is not dependent on the purity, the reason for the difference in the alloys ought to be sought in the high binding energy of chromium and carbon (and/or nitrogen). However, the pre-passivation stage is not modified. This means that the impurities in the solid solution influence the active dissolution of the naked surface of the metal and their action is impeded when a layer is formed.

It is possible to explain why carbon is able to promote a large shift in the activity potential in the positive direction by considering the thermodynamic activity of chromium in relation, to the chromium content on one hand and, the carbon content on the other. Fig. 4 shows plots of two types of curve, based on recent data [2]: a_c in relation to the chromium content (Fig. 4a) and a_c in relation to the carbon content (Fig. 4b). Comparison of two curves shows that a_c undergoes the same modification by a decrease of chromium content from 9% to 4% or an increase of carbon content from 50 to 62 ppm. The chromium activity is deduced from the carbon activity by considering the following thermodynamic hypothesis: in a ternary alloy as Fe–Cr–C in which the interaction between Cr and C is very strong compared with that between Fe and Cr or Fe and C [7] we can apply the Gibbs–Duhem formalism:

$$X_{Cr} \, d \log a_{Cr} = -x_C \, d \log a_c$$

$$d a_{Cr} = -\frac{\gamma_{Cr}}{\gamma_C} d a_c$$

γ_{Cr}/γ_C can be evaluated from 1 to 3 [8].

For our present purpose, this means that a_{Cr} decreases by the the same amount as (1) the chromium content decreases by 5%, or (2) the carbon content increases by only 12 ppm; and for a long time, it has been well known that a decrease in a_{Cr} involves a positive shift of the anodic curve. Thus, a few ppm of carbon are able to promote a large shift in the activity peak E_1. On the other hand, variation of chromium content affects the active dissolution E_1 only slightly but has a great effect on the pre-passivation stage (Fig. 3).

3.2. Effect of segregation on anodic curves

By comparing the solid solubility of carbon at 780° C, i.e. 15 ppm [2], with the carbon content of alloys E and P, it seems likely that segregation occurs mostly for P alloys after recrystallization.

3.2.1. Microstructural study

The examination of thin foils in the electron microscope shows:

(1) for alloys E, all the boundaries were well equilibrated. They were perpendicular to the free surface of the foil, even in thicker parts and, by tilting, only thickness fringes were revealed;

(2) for impure alloys P, although the isothermal holding time at 780° C was very long, the samples were not completely recrystallized. Many boundaries presented particular structural features which looked like extrinsic defects [9–11] (Figs. 5 and 6). Along these boundaries a white zone was often present, and sometimes nitrides or oxides were embedded at their interface with the bulk (Fig. 7a and b). These boundaries called "interfaces with extrinsic structure" (ISE) [12].

Sometimes the width of these interfaces was very large (Fig. 8) and it seemed necessary to prove that they were really interfaces; this verification could be done by tilting the specimen in the

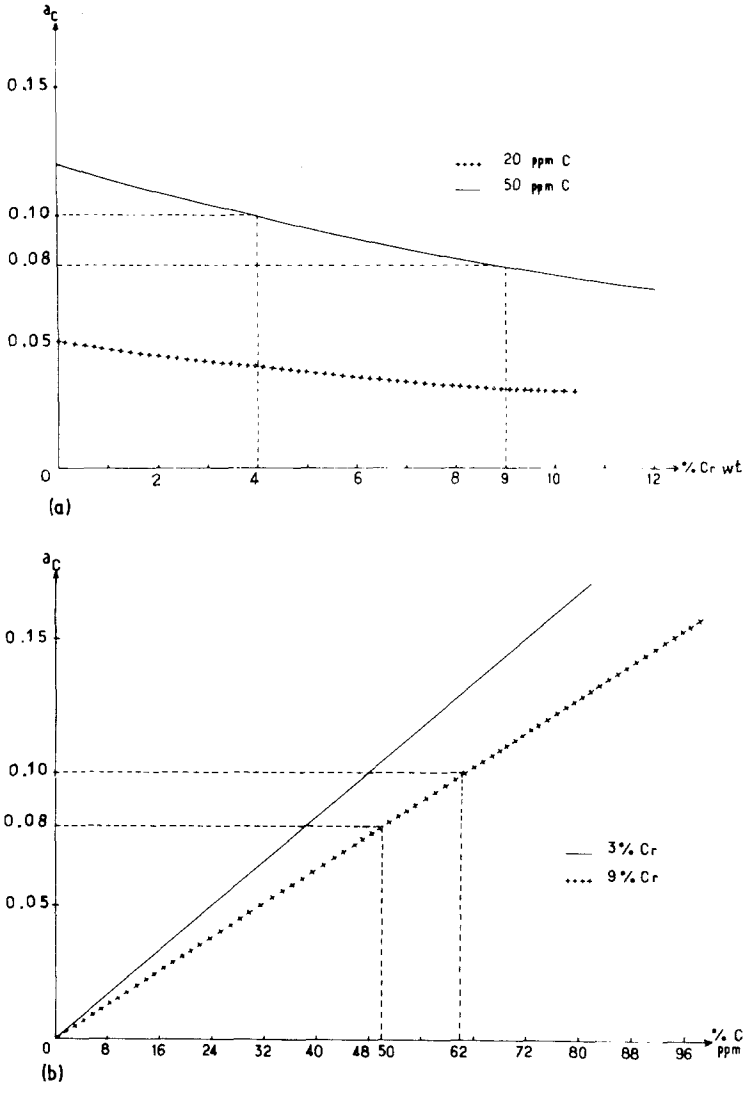

Figure 4 Variation in the activity of carbon at 800°C in relation to (a) the chromium content (the alloys contain, respectively, 20 and 50 ppm carbon; (b) the carbon content (the alloys contain, respectively, 3 and 9% chromium).

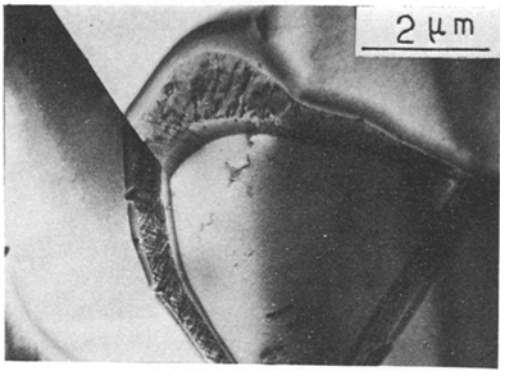

Figure 5 Extrinsic defects in grain boundaries (100 kV).

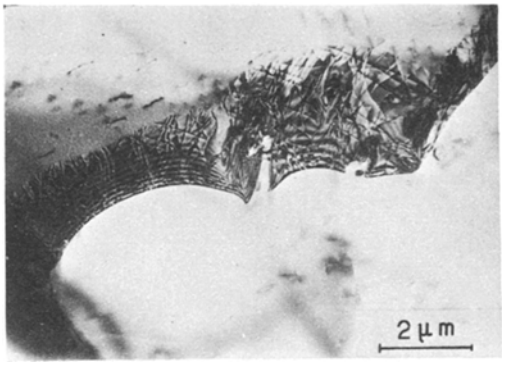

Figure 6 Interface with extrinsic defects observed at 1000 kV.

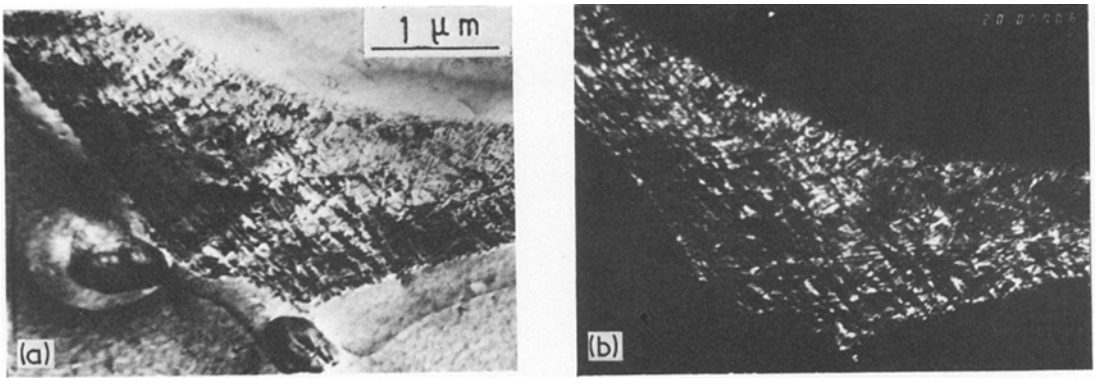

Figure 7 Presence of white areas along the ISE and nitrides at its limit with the bulk. (a) Bright-field image; (b) dark-field image obtained from a double diffraction spot.

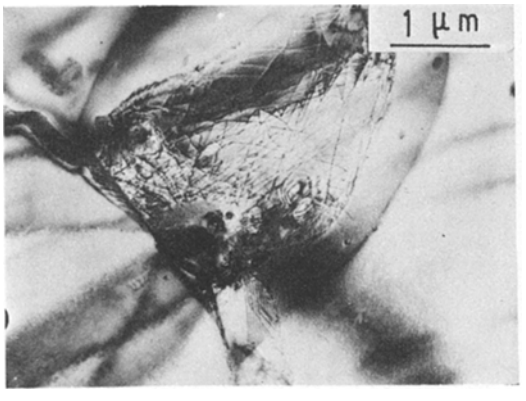

Figure 8 Very "broad" interface in a sample recrystallized for 10 min at 780° C.

electron microscope or by comparing the STEM with the SEM images (Fig. 9).

By probing the chromium content in the STEM, no difference between the boundaries, the white areas along them, and the bulk could be found. All attempts to detect microprecipitates in these interfaces were unsuccessful.

The observations of high-resolution autoradiography of ^{14}C on replicas of samples containing a little more carbon revealed a higher concentration of silver filament detecting an over-concentration of carbon in broad boundaries (Fig. 10a). On thin foils, the interfaces with defects and nitrides seem to gather silver grains (Fig. 10b).

Thus, from a microstructural point of view, the greatest difference between alloys E and P was the presence of interfaces containing many defects, most probably carbon segregation and, sometimes, precipitates.

3.2.2. Electrochemical study

The anodic behaviour of both alloys was then compared. For pure alloys E, the anodic curve remained identical to that of homogenous alloys previously studied. However, for impure alloys P, the anodic curve of recrystallized samples presented a new fact, that is, the appearance of an intermediate peak between E_1 and E_2 (Fig. 11).

The obvious idea is to relate this peak to the boundaries with defects (carbides and nitrides) and to attempt to distinguish between these parameters, to this purpose, the following experments were carried out.

(1) taking the pure alloys, either 50 ppm carbon or 50 ppm nitrogen were added. In the case of

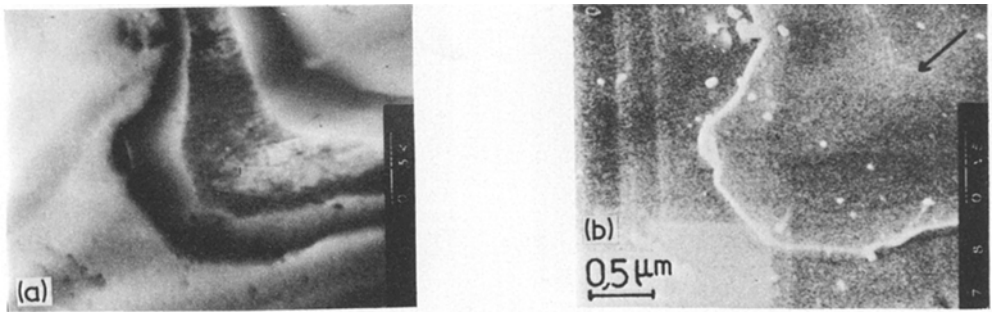

Figure 9 Observation of an ISE: (a) in STEM; (b) in SEM (the second limit, see arrow, is very weak.)

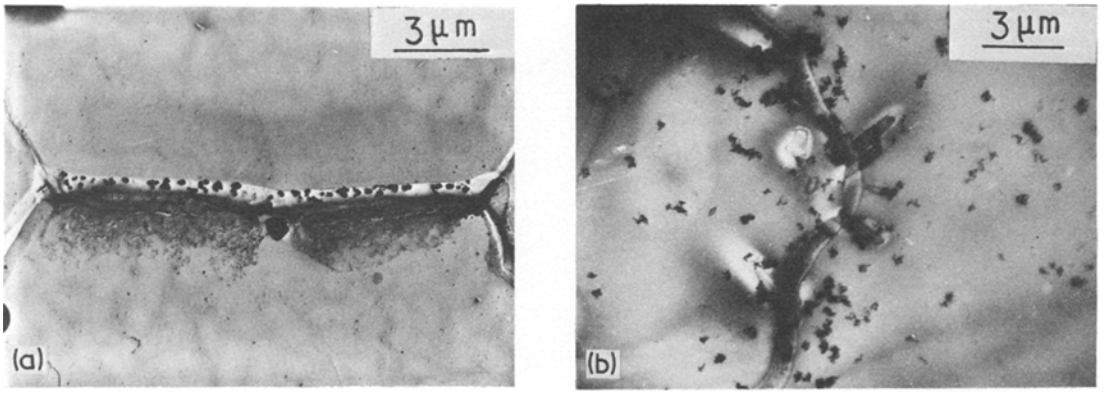

Figure 10 Autoradiography HPR of ^{14}C showing an overconcentration of silver filaments on some boundaries: (a) observation on replica; (b) observations on thin foil.

carbon, the observations showed the appearance of complex interfaces and, at the same time, the appearance of an intermediate peak on the anodic curve. In the case of nitrogen, no special features appeared in boundaries apart from nitrides at higher concentrations, and there was no intermediate peak on the anodic curve. Thus nitrogen plays no role.

(2) Different isothermal holding times at 780° C were performed: 10 min, 3 h, 3 and 22 days. Even after 22 days, the presence of ISEs could not be avoided but their density decreased slowly with time. Simultaneously, the intensity of the intermediate peak decreased. (Fig. 12). On the reverse curve, plotting with decreasing potential from the passivation step, it must be pointed out that the intermediate peak never appeared.

(3) By etching the samples at the suitable intermediate peak, the ISEs were preferentially attacked (Fig. 13).

(4) The anodic curves of pure carbides and pure nitrides showed that they cannot influence the activity region of these curves [12].

3.2.3. Interpretation

All the results emphasize the relation between E_{int} and special features in grain boundaries including carbon segregation. The appearance of the intermediate peak can be interpreted on the basis of the previous result concerning the role of carbon in solid solution. Indeed, despite the low carbon content in alloys P (50 ppm), the high value of the β enrichment factor recently calculated by Hondros and found to be of the order of 300 at 800° C [13] can explain a large amount of carbon in grain boundaries and, more probably, in

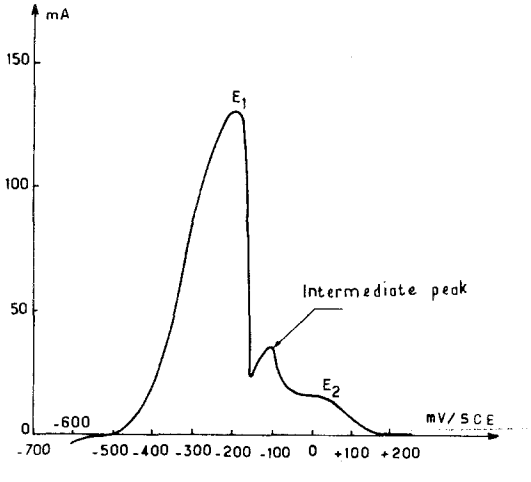

Figure 11 Anodic curve of an Fe 9% Cr alloy P, recrystallized 3 days at 780° C.

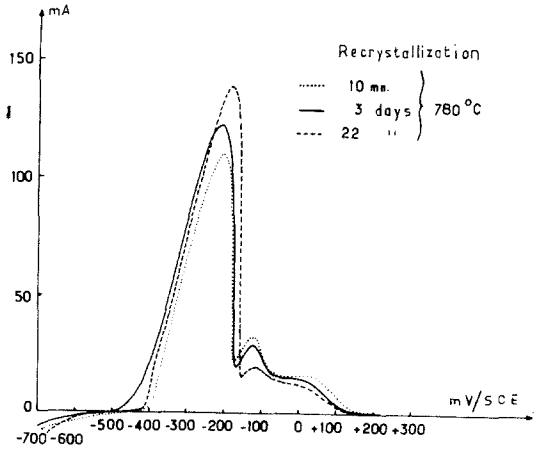

Figure 12 Variation of the intensity of the intermediate peak with different holding times at 780° C.

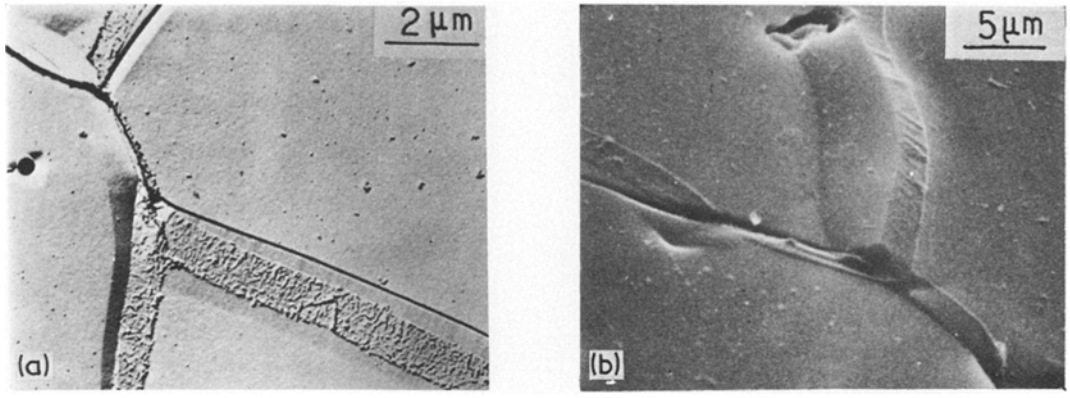

Figure 13 Observation of the selective attack of the ISE at the intermediate peak: (a) on replica by STEM; (b) on thick sample by SEM.

complex boundaries, as recent studies led to the trend of trapping interstitials by extrinsic defects [14]. Thus carbon very localized in the ISE involves a positive shift of the activity peak of these areas; the potential E_1 remains the activity peak of the bulk, the intermediate peak is the activity peak of the interfaces with carbon segregation.

However, when the protective layer is formed at higher potentials, its coating is not affected by these very small areas (10 Å about the grain-boundary plane). This is the reason why, on the reverse curve, the passive layer is not destroyed until the E_1 of the bulk is reached, and there is no intermediate peak [15].

The previous explanation of the appearance of the intermediate peak relies upon the elemental form of carbon (or clusters). However, so far there is no direct proof of the chemical state of carbon. Because of the shortcomings of the techniques, it is not possible to avoid the presence of depleted chromium microareas surrounding microprecipitates not detectable by STEM. The aim of the last part of this paper is to answer this question by purposefully making samples with precipitates and dechromized areas and looking at their anodic behaviour.

3.3. Anodic behaviour of dechromized areas surrounding precipitates

3.3.1. Structural observations

The ferrite obtained by slowly cooling the alloys from 1000° C to room temperature contains many inter and intra-granular carbides and nitrides and complex interfaces (Fig. 14). The diffusion coefficient of chromium in alloys is too small to avoid depletions around these precipitates, which have been detected by STEM microanalysis (Fig. 15).

The presence of ISEs can be understood, because the phase transformation $\gamma \rightarrow \alpha$, requires the mobility of interfaces which is impeded by carbon. This possibility is enhanced for α/γ boundaries as a result of the great difference of the limit solubility of carbon in the two phases. It is well known that carbon is ejected from the new phase α to the α/γ boundary during the transformation [16].

To compares with the previous microstructure, sensitized alloys without ISEs were prepared by holding quenched samples at 550° C for 15 min.

3.3.2. Electrochemical behaviour

The anodic behaviour of these alloys is compared with that of the homogeneous and recrystallized samples P (Fig. 16a). For alloys displaying ISEs and depleted chromium areas (treatment C), the

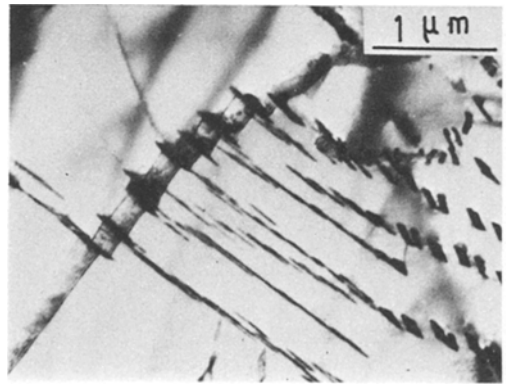

Figure 14 Precipitates and ISE in an alloy slowly cooled from 1000° C.

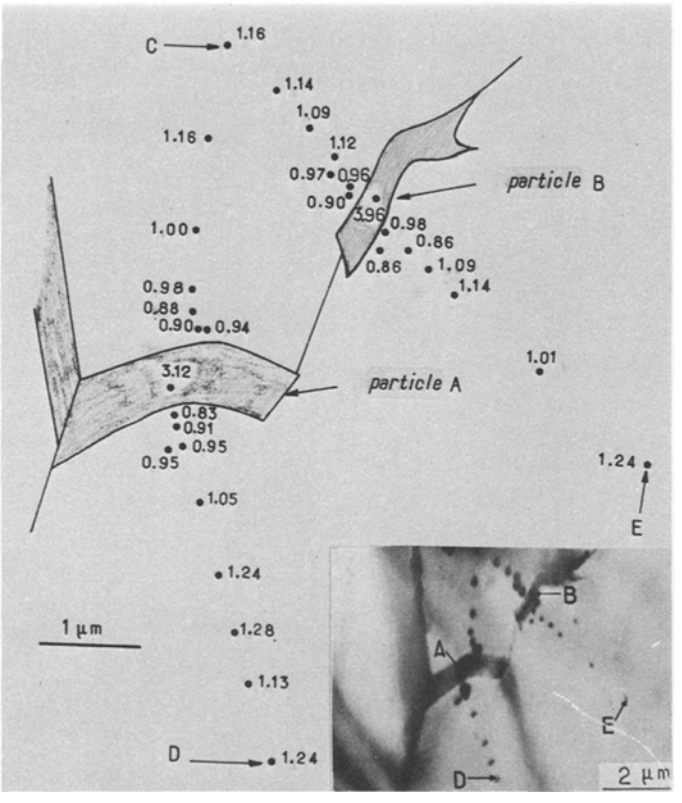

Figure 15 Depletion of chromium around carbides detected by microanalysis by STEM. (The results are given in Cr/Fe X 10; the analysed points can be seen on the micrograph.)

curve still presents an intermediate peak but there is a new factor: the intensity of E_2, very weak for homogeneous alloys is now relatively high. It seems likely that E_2 can be attributed to the depleted chromium areas. This hypothesis is confirmed by looking at the curve of the sensitized alloys: only E_2 is present.

According to the role of the chromium content, it is not surprising that the dechromized areas affect the passivation stage much more than the active dissolution. The pre-passive and passive layers are modified; this fact can be seen more clearly on the reverse curves (Fig. 16b): the destruction of the passive and the pre-passive layers needs high intensity [17]. This phenomenon is well known as "reactivation" [18].

Taking into account the comparative effects of chromium and carbon described previously, it is to be expected that the shift of E_1 due to a depletion of chromium must be less important than its shift due to an enrichment of carbon. In point of fact, the E_1 of samples containing dechromized areas is only slightly more positive than E_1 of the bulk; the difference is clearly revealed on the reverse curve when this peak is reactivated.

4. Conclusion

From a structural point of view, this work shows that a thorough electro-chemical study of some alloys could be a possible means of detecting grain-boundary segregation of carbon, whereas no microanalysis can yet achieve this. Providing the possibility to separate the effects of a segregation on the formation and the destruction of passive film from those of a precipitation, the results strongly suggest that the chemical state of carbon in interfaces with extrinsic structure (ISE) ought to be an elemental form (or cluster). In contradiction to the observations of other authors [19] the high stability of the extrinsic defects in grain boundaries, even after long recrystallization treatment, can be interpreted as the result of a strong interaction between interstitials and these defects, as pointed out by Li [20] and Varin *et al.* [10].

From a corrosion point of view, it seems highly likely that some boundaries displaying carbon segregation could be microareas in which the chromium activity, depending on the carbon content, is very low compared with that of the bulk. Their corrosion rate is higher; despite the absence of precipitates, they constitute very active

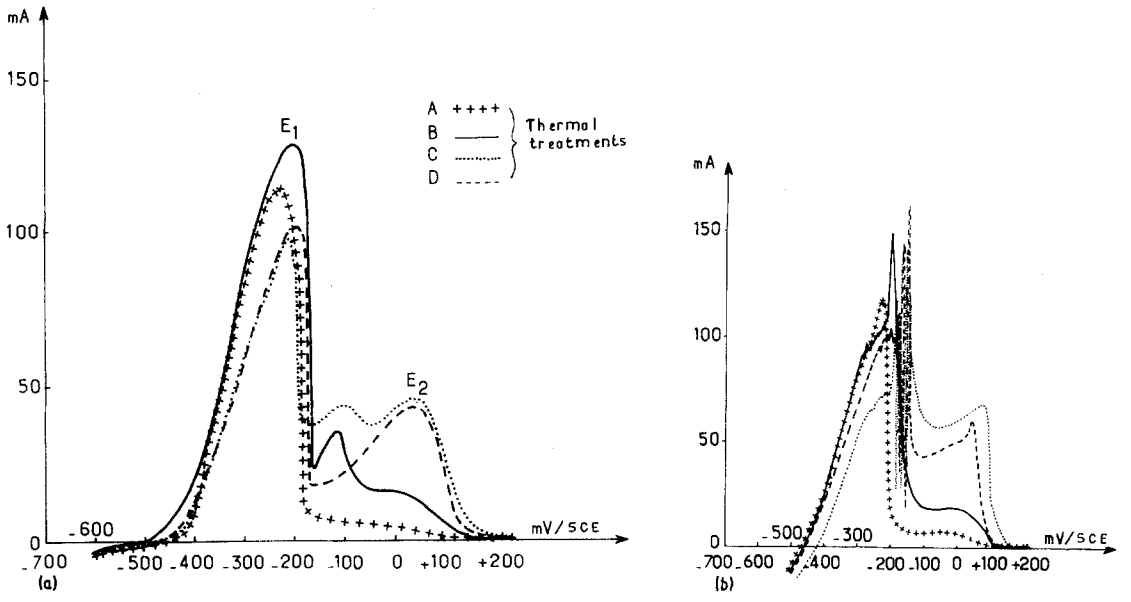

Figure 16 Anodic curves of Fe 9% Cr (a) direct curves; (b) reverse curves. A, homogeneous; B, ISE + segregations; C, ISE + depleted chromium areas; D, sensitized.

micropiles at the surface and can give rise to sharp intergranular corrosion.

References

1. E. D. HONDROS, "Grain boundary structure and properties" (Academic Press, London, 1976) p. 265.
2. R. LUNDBERG, M. WALDENSTROM and B. URHENIUS, *Calphad* **1** (1977) 159.
3. M. FROMENT, P. MOREL and J. EPELBOIN, *Mém Sci. Rev. Mét.* **59** (1962) 225.
4. A. A. EL MILLIGY, D. GEANA and W. T. LORENZ *Electrochem. Acta* **20** (1975) 273.
5. C. L. McBEE and J. KRUGER, *ibid* **17** (1962) 1337.
6. J. P. LAURENT and G. LAPASSET, *Int. J. Appl. Rad. Isot.* **24** (1973) 213.
7. M. GUTTMANN, *Le vide et les couches minces* **177** (1975) 43.
8. C. S. TEDMON, D. A. VERMILYEA and J. H. ROSOLOWSKI, *J. Electrochem. Acta.* **118** (1971) 192.
9. J. P. HIRTH and R. W. BALLUFFI, *Acta Met.* **21** (1973) 929.
10. R. A. VARIN, J. A. KUZUBOWSKI and N. W. GRABSKI, *J. Phys.* **36** (1975) 43.
11. D. BOUCHET, L. PRIESTER and P. LACOMBE, *J. Microsc. Spectrosc. Electron.* **1** (1976) 327.
12. D. BOUCHET, *Thèse Orsay*, March (1978).
13. E. D. HONDROS and M. P. SEAH, *Met. Trans.* **8A** (1977) 1363.
14. B. RALPH, *J. Phys. 36* (1975) 117.
15. D. BOUCHET, L. PRIESTER and P. LACOMBE, *Compt. Rend. Acad. Sci. Paris* **284** (1977) 415.
16. G. MOULIN, B. LESAGE, L. PRIESTER and A. M. HUNTZ, *Metallogr.* **11** (1978) 81.
17. D. BOUCHET, L. PRIESTER and P. LACOMBE, *Mém. Sci. Rev. Mét.* **74** (1977) 709.
18. V. CIHAL, A. DESESTRET, M. FROMET and G. H. WAGNER, Communication au 5éme Congrés Européen de Corrosion, Paris (1973) p. 249.
19. A. R. JONES, P. R. HOWELL and B. RALPH, *Phil. Mag.* **35** (1977) 603.
20. J. M. C. LI, *Trans. AIME* **227** (1963) 239.

Received 12 December 1978 and accepted 22 January 1979.